We are IntechOpen, the world's leading publisher of Open Access books Built by scientists, for scientists

7

Shape Measurement by Phase-Stepping Method Using Multi-Line LEDs

Yoshiharu Morimoto[1], Akihiro Masaya[1],
Motoharu Fujigaki[2] and Daisuke Asai[3]
[1]Moire Institute Inc.,
[2]Wakayama University,
[3]Hikari,
Japan

1. Introduction

Three-dimensional shape measurement is used in various fields such as robotics and inspection of industry production. It is requested to measure shape with high speed and high accuracy. It is also requested to make the system compact and low-cost. It is, however, difficult to satisfy these requests simultaneously for 3D shape measurement. In order to measure shape in real-time, Kato et al. proposed a method using phase-shifting electronic moiré pattern (Kato et al., 1997). The authors developed integrated phase-shifting method for real-time shape measurement by a grating projection method using phase-shifting (Morimoto et al., 1999, Fujigaki & Morimoto, 2003). However, they showed only the phase distribution of the contour lines.

In almost all conventional shape measurement methods, the optical systems are modelled and the parameters of the model are obtained with a calibration process using calculation of the geometrical parameters of optical devices such as positions of lens centres of a camera and a projector. However, the model cannot contain all of the information of the optical system such as lens distortion, intensity error of a projected grating, brightness linearity of a projector and a camera, etc. The less information causes measurement errors. Furthermore, it is time-consuming to calculate the spatial coordinates using the parameters.

In order to obtain a 3D-shape with grating projection method, the authors previously proposed whole-space tabulation method (WSTM) (Fujigaki & Morimoto, 2008a, Fujigaki et al., 2008b, 2009, Morimoto et al., 2009). The relationship between the coordinates and the phase of the grating recorded at each pixel of a camera is obtained as calibration tables in a three-dimensional space by experiment beforehand. Therefore the analysis is very fast because of looking at the calibration tables from the phase information at the pixel without any complex calculation. It provides fine resolution even when the phase distribution of the grating is not linear.

The tabulation method is extended to a case of inaccurate phase-shifting of a grating by a projector using five-line light emitted diode (LED) light sources (Morimoto et al., 2010a, 2010b). In this paper, a grating projector with nine-line LED light sources is newly developed. The phase-shifting usually uses a grating projector with a high resolution stage or a liquid crystal display (LCD) projector. It is expensive and limits the speed of phase-shifting. The light-power efficiency of an LED is very high. The size of the light source is very small. It is easy and very fast to control the power and the switch on/off timing. The nine-line LED light sources are set in front of a grating. The switch for each LED line of the light sources is 'switch on'. The phase of the grating shadow is shifted by changing the switches for LEDs into 'on/off' in synchronization with the phase-shifting and the recording with the camera sequentially. Using the LED light sources for a grating projector, it is possible to make phase-shifting without any moving devices. The projector is low cost and high-speed. The authors call the method 'phase-stepping method using multi-line LEDs.' Even when the positions of the LED light sources are not so accurate, the error is almost cancelled by using the calibration tables obtained by the WSTM with the same experimental setup. This method will satisfy for shape measurement system high-speed, high accuracy, compact and low-cost.

In this paper, the theory and the system of shape measurement using the WSTM and the phase analysis methods using multi-line LED light-sources are explained. Furthermore, some experimental results of shape measurements using the system are shown.

2. Phase-shifting method in grating projection method

2.1 Grating projection method

Figure 1 shows a schematic system for grating projection method. A grating with a cosinusoidal brightness distribution is projected by a projector. The grating projected on an object is deformed according to the shape of the object. The deformed grating is recorded by

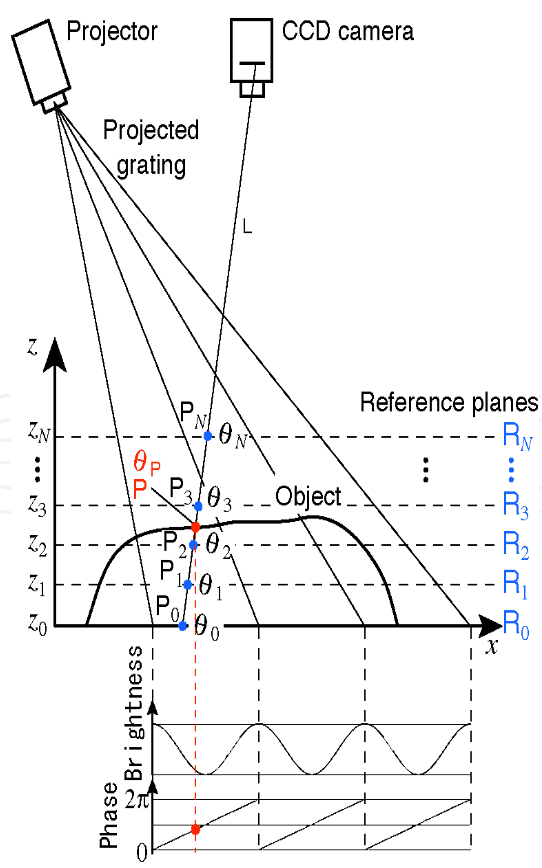

Fig. 1. Schematic view of grating projection system

a camera and analyzed the deformed grating to obtain the shape. As analysis method of the deformed grating, phase shifting method which is the most popular accurate method, is used as mentioned next section.

2.2 Phase-shifting method

In shape measurement using grating projection method, phase analysis of the projected grating provides accurate results. In order to analyze the phase, there are many methods (Takeda & Mutoh, 1983, Asundi & Zhou., 1999, Sitnik & Kujawinska, 2002, etc.). Phase-shifting method is the most popular method. Let us explain the phase-shifting method. Figure 2(a) shows phase-shifted grating patterns projected onto an object. Figure 2(b) shows the brightness (intensity) distributions along the horizontal center line of Fig. 2(a). The intensity distribution is almost cosinusoidal.

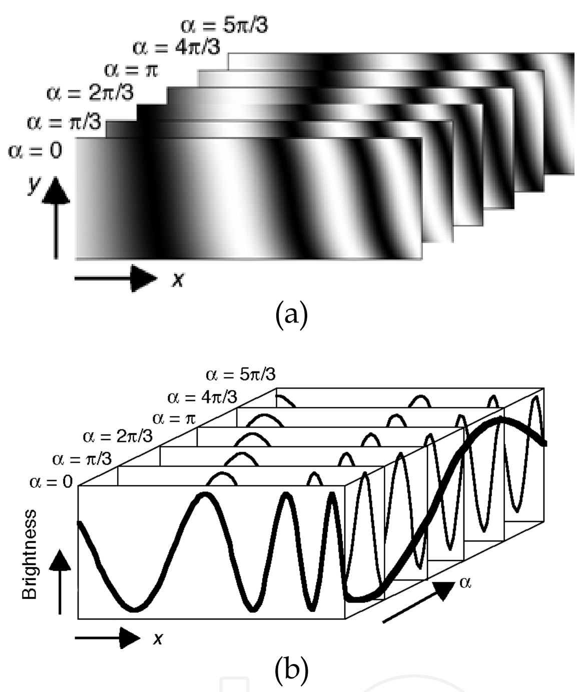

Fig. 2. Phase analysis of projected grating using phase-shifting grating images; (a) Phase-shifted grating pattern projected onto object; (b) Brightness distribution along horizontal center line of Fig. (a)

When a grating with a cosinusoidal brightness distribution is projected or displayed on a reference plane or an object, and the phase of the grating is shifted N times for one cycle, the k-th phase-shifted grating images can be expressed as follows:

$$I_k(x, y) = I_a(x, y)\cos[\theta(x, y) + k\frac{2\pi}{N}] + I_b(x, y) \quad (k = 0,1,\ldots, N-1) \tag{1}$$

where $I_b(x, y)$ represents the background brightness in the image, which is insensitive to the change in phase. $I_a(x, y)$ represents the amplitude of the grating brightness and $\theta(x, y)$ is the initial phase value. The phase distribution of the grating pattern can be obtained as follows (Srinivasan et al., 1984, 1985).

$$\tan\theta(x,y) = -\frac{\sum_{k=0}^{N-1} I_k(x,y)\sin(k\frac{2\pi}{N})}{\sum_{k=0}^{N-1} I_k(x,y)\cos(k\frac{2\pi}{N})} \quad (2)$$

Usually N is selected as 3 or 4. If the number N of the phase-shifted moiré patterns is larger, the phase analysis becomes more accurate. In this study, N =4 and 6 are selected.

3. Whole-Space Tabulation Method (WSTM) (Fujigaki et al., 2008a, 2008b, 2009, Morimoto et al., 2009)

In grating projection method, the coordinates of a point on an object is usually calculated using the geometric positions of the lenses of a camera and a projector. If the distortion of lenses is considered, the calculation is complex and time-consuming. Therefore several methods using a reference plane or reference planes were proposed for accurate shape measurement (Zhou & Su, 1994, Asundi & Wensen, 1999, Su et al., 2004, Ha et al., 2004, Yen et al., 2006). For real-time shape measurement, it is required to calculate spatial coordinates from the phase values of the projected grating in short time. The authors previously proposed the calibration methods which used two or multiple reference planes (Fujigaki & Morimoto, 1996, Shinke et al., 2001, Ri et al., 2005). The calibration method was extended to a very large number of planes. All the relationships between the phase of the projected grating and the spatial coordinates can be obtained as calibration tables for each pixel of the camera. The method is called 'whole-space tabulation method' (WSTM). Let us explain the method.

Figure 1 also shows a schematic view of a shape measurement system by grating projection method and explanation of the principle of the calibration method using multiple reference planes. An LCD panel as a reference plane is set on a linear stage. The LCD panel is covered with a scattered film. The scattered film functions as a screen when a grating pattern is projected from the projector onto the reference plane. It is used to make calibration tables on the relationship between the phase θ and the z coordinate. The scattered film also functions as a backward screen when a grating patterns are displayed on the LCD panel to determine the x and y coordinates.

The LCD reference plane is set vertically to the z-direction. It is translated in the z-direction step by step. A camera and a projector are arranged and fixed in front of the reference plane. The grating is projected on the reference plane at first, and it is also projected on an object to be measured later. By translating the reference plane along the z-axis, a pixel of the camera records the intensities as images at the points P_0, P_1, P_2 …. and P_N, on the reference planes R_0, R_1, R_2…. and R_N, respectively. And also, by recording the phase-shifted grating images, the phase distribution along the visual line L of a pixel of the camera is obtained.

In order to obtain the x and y coordinates on the reference plane, the phase-shifted gratings displayed on the LCD panel are taken by the camera. From these phase-shifted images, the calibration tables are formed to obtain the x, y and z coordinates from the phase θ at each pixel as shown in Figs. 3 and 4.

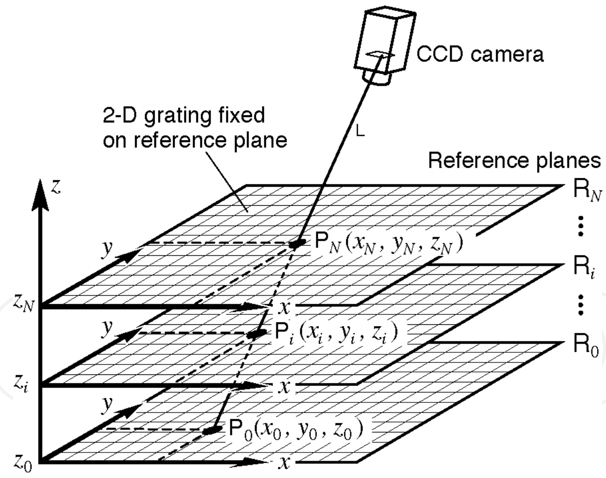

Fig. 3. Schematic view of calibration tables to obtain *x, y* and *z* coordinates from phase in whole space tabulation method

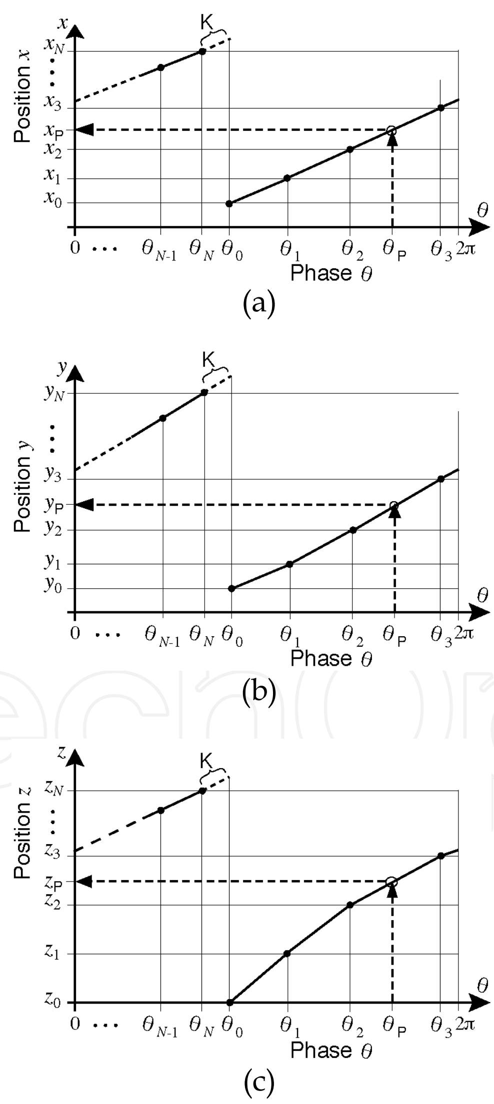

Fig. 4. Calibration tables to obtain *x, y* and *z* coordinates from phase at each pixel point of camera; (a) Table of phase θ and *x;* (b) Table of phase θ and *y;* (c) Table of phase θ and *z*

In the measurement procedure, an object is placed between the reference planes R_0 and R_N. Phase-shifted gratings are projected onto the object and the phase distributions of the grating are analyzed from the phase-shifted grating images. The 3-D coordinates at each pixel are obtained from the phase value in high-speed by referring the calibration tables for each pixel.

This method is called the WSTM as mentioned already. It excludes the effect of lens distortion and intensity error of the projected grating in measurement results theoretically. Tabulation makes short-time measurement possible because the 3D coordinates are obtained by looking at the calibration tables from the phase at each pixel point of the camera and it does not require any time-consuming complex calculation.

4. Phase-stepping method by changing light sources

4.1 Geometrical relationship among phase, phase-stepping amount and intensity of projected grating

Let us explain the principle of the phase-stepping method using multi-line LED light sources. Figure 5 shows that a grating is projected from the light sources. This figure shows in the case of four line LED light sources. If each line LED light source is switched on and off one by one sequentially, the shadow of the grating is moved.

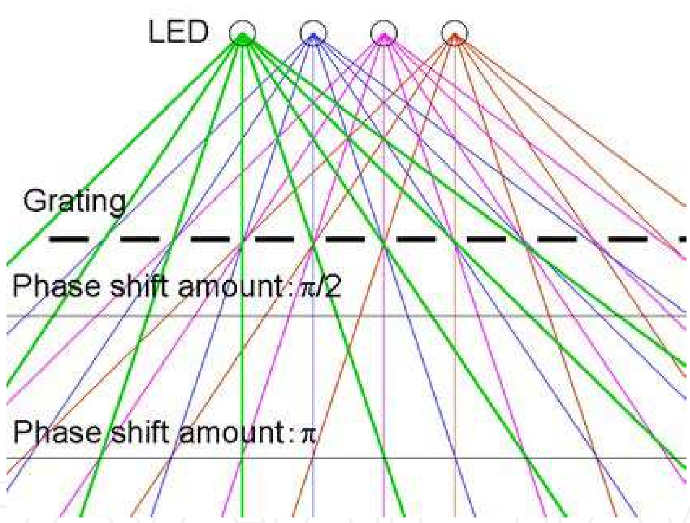

Fig. 5. Shadow of grating is moved when each line LED is switched on and off one by one sequentially. Phase stepping amount is function of vertical distance from LED light source in phase-stepping method using multi-line LED light sources

The amount of phase shifts changes with the z-directional distance from the light source to each point in Fig. 5. The positions with the amounts of phase shift, $\pi/2$ and π, are shown as horizontal straight lines, respectively.

The equations of the geometric relationship among light sources, a grating and an object are derived using Fig. 6. In this figure, five line LED light sources are shown as an example. Now, the subscript number n is given to each line LED light source L, and the *n*-th line light source is set to L_n (n=0, 1, 2, 3, 4). The light sources are mutually parallel and the five lines have regular intervals with the pitch *l*. The plane including the five LED line light sources is

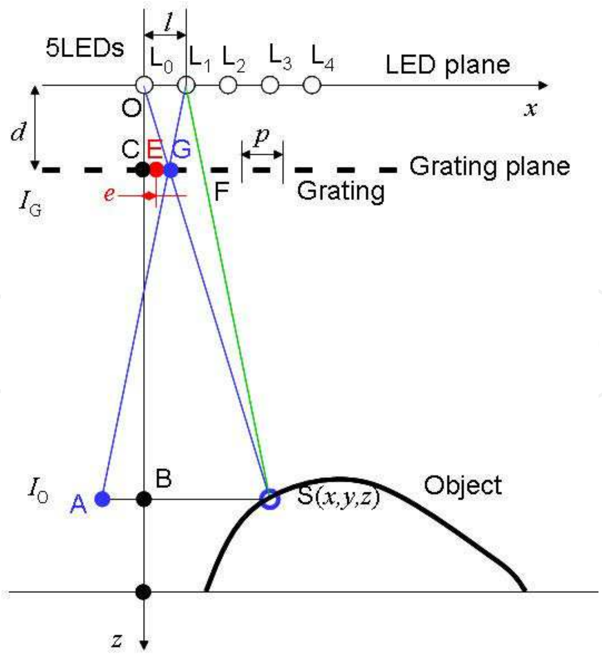

Fig. 6. Schematic of grating projection system and object in shape measurement system using five line LED light sources

called an LED plane where z=0 with the field (x, y). The position of the first LED line L_0 is the origin O of the x, y, and z coordinates. In the LED plane, the x direction is normal to the LED lines, and the y-direction is the parallel to the LED lines. The z-direction is normal to the LED plane. The brightness distributions of the five line LEDs are assumed as uniform and equal in the x- and y-directions in the observation region at fixed z.

A grating plane is parallel to the LED plane, and the distance between the LED plane and the grating plane is d. The grating lines with pitch p drawn on the grating plane are parallel to the LED lines. The intersection of the grating plane and the z-axis is set to C and the distance between C and the origin E, i.e., the center E of the first grating line is set to e.

The transmissivity intensity distribution of the grating at z=d is denoted by the following equation.

$$I_g = a_g \cos\{\Phi\} + b_g = a_g \cos\{\frac{2\pi}{p}(x_g - e)\} + b_g \tag{3}$$

where Φ is the phase, a_g is the amplitude, b_g is the intensity of background, x_g is the x-directional coordinate at the grating plane, that is, x_g is the x-directional distance from the point C.

When the light source L_0 is switched on and the shadow of the grating is projected at the position S(x, y, z), the intensity at the position S(x, y, z) is expressed by the following equation.

$$I_0 = a_g \frac{d^2}{z^2}\cos\{\frac{2\pi}{p}(\frac{d}{z}x - e)\} + b_g \frac{d^2}{z^2} \tag{4}$$

where it is considered that the intensity at a point is inversely proportional to the square of the distance z. As shown in Fig. 6, the point G of the grating is projected at the point S on the object. Only the n-th line LED light source L_n is switched on one by one, and it is considered that the shadow of the grating is projected on the object.

The intensity distribution of the shadow projected through the grating from the light source L_n has the following distribution shown at z.

$$I_n = a_g \frac{d^2}{z^2} \cos[\frac{2\pi}{p}\{(\frac{d}{z}x - e) + nl(1 - \frac{d}{z})\}] + b_g \frac{d^2}{z^2} = a\cos\{\Phi + n\Psi\} + b \tag{5}$$

where

$$a = a_g \frac{d^2}{z^2} \tag{6}$$

$$b = b_g \frac{d^2}{z^2} \tag{7}$$

$$\Phi = \frac{2\pi}{p}(\frac{d}{z}x - e) \tag{8}$$

$$\Psi = \frac{2\pi l}{p}(1 - \frac{d}{z}) \tag{9}$$

4.2 Relationship among phase, phase-shift amount and height

When the shift amount Ψ is obtained, the z-coordinate is determined using Eq. (9) as follows.

$$z = \frac{2\pi ld}{2\pi l - \Psi p} \tag{10}$$

When the phase Φ is obtained, the z-coordinate is determined using Eq. (8) as follows.

$$z = \frac{2\pi dx}{p\Phi + 2\pi e} \tag{11}$$

From Eq. (10) or (11), the z-coordinate is obtained.

4.3 Phase analysis by phase-stepping method by changing light sources

As shown in the case of $\Psi=\pi/2$ and $\Psi=\pi$ in Fig. 5, there are the positions where the phase shift amounts are $2\pi/N$ (N is an integer). At the positions, the phase analysis becomes possible using Eq. (2). At the other positions, there are some errors in the phase value obtained using Eq. (2). However, if the relationship between the calculated phase θ and z is a single-valued function at some region, the phase determination is possible in the region by combining the WSTM. The height is exactly obtained by looking up the tables of the WSTM even if the phase shifting method has a little error.

5. Experiment

5.1 Experimental setup

In this study, some experiments are performed to confirm the performance of the phase-stepping method using line LED light sources. Figure 7 shows the schematic optical system of the experiment. Figure 8 shows the photograph of the LED board with 9 line LED light sources we developed.

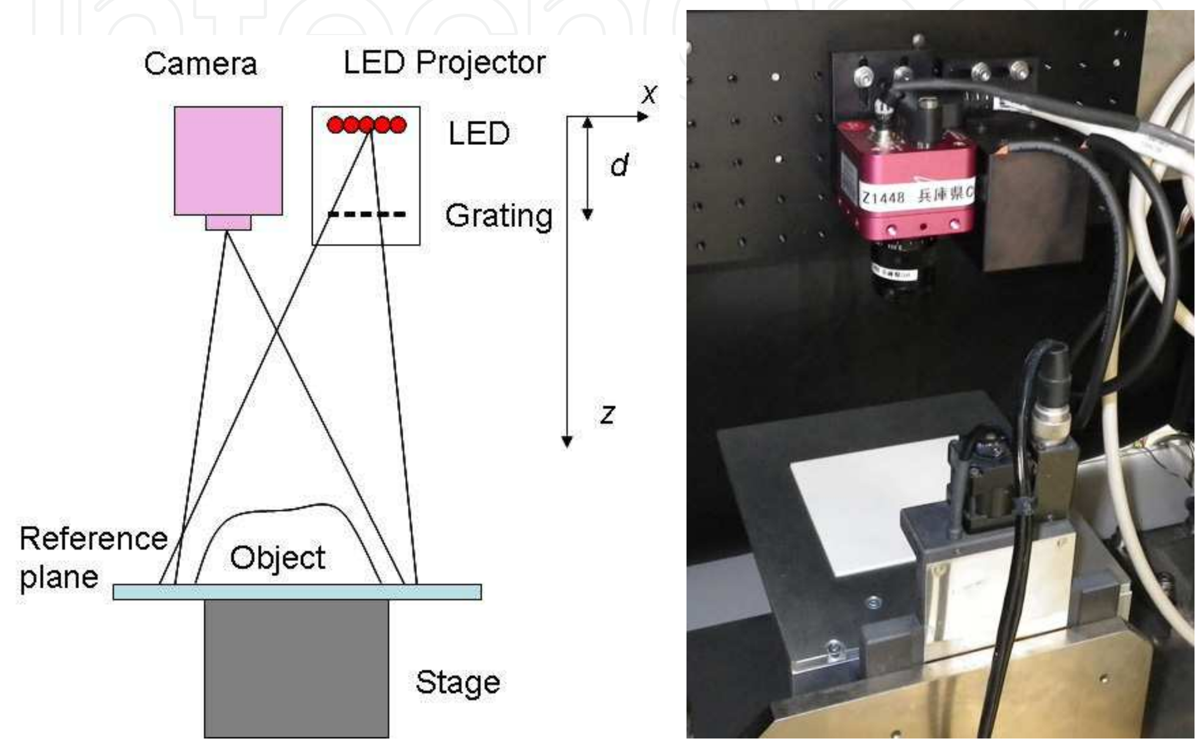

(a) (b)

Fig. 7. Optical system used in experiment; (a) Schematic view; (b) Photograph

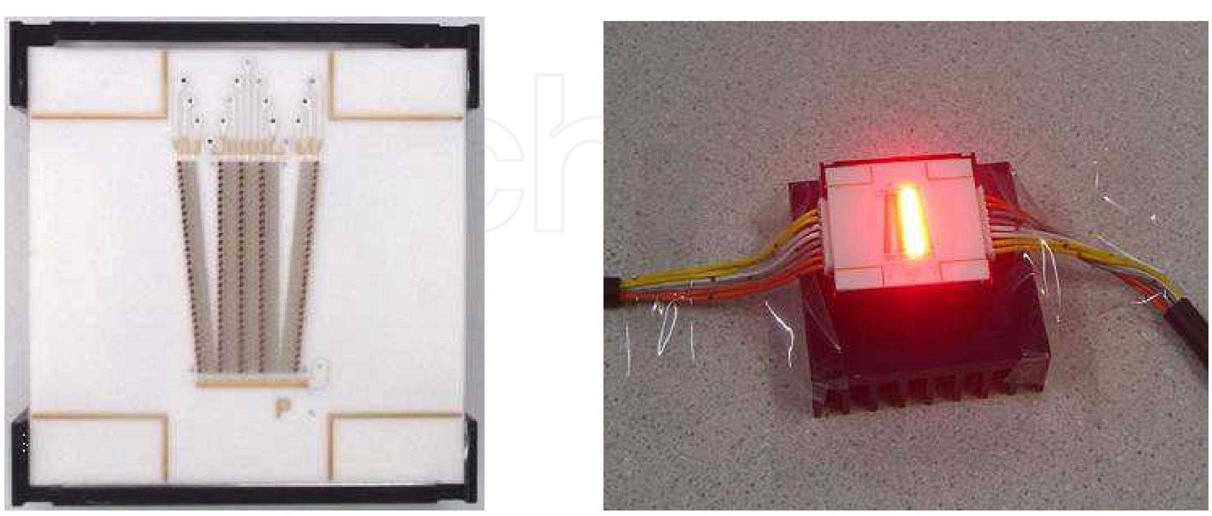

(a) (b)

Fig. 8. Photographs of the developed line LED light sources; (a) Board with 9 LED lines and slanting 6 lines; (b) Photo when switching on a line

The LED has nine lines perpendicular to an x-axis, and slanting six lines. Here, the perpendicular lines are used. The pitch l of the LED lines is 0.5 mm. One line has 30 LED tips of a 0.35-mm square. A Ronchi grating is used as a grating. The pitch p of the grating is 0.5 mm. The interval d between the LED plane and the grating plane is 30 mm. The experiments are performed where the base level of z is 180 mm.

5.2 Experimental results

The experimental results were shown in Figs. 9 to 14.

Figure 9 shows the intensity distributions in the x direction in the center of the y direction of the grating projected on the reference plane when the lighting line LED light sources were changed. In this figure, only five distributions are shown. .Although there is some random noise, the intensity distributions are almost cosinusoidal and the phase shift is also performed at equal intervals. Although this random noise is decreased by time averaging, any averaging is not used in this study to confirm the performance.

At first, only the first four lines of LED were used for the phase-stepping method and the phases are calculated using N= 4 in Eq. (2). The phase distribution along the x-axis on the reference plane at z=180mm is shown in Fig. 10(a). Although the phase distribution is repeated from $-\pi$ to π several times, the relationship between z and phase at a point of the reference plane for a 2π phase interval is shown in Fig. 10(b). The relationship is considerably curved although the relationship is almost straight line in theoretical treatment. However, by combining the WSTM, the errors will be cancelled by using the same optical system when the tables are used. Then the measurement is performed during a 2π phase interval without unwrapping of phase.

In the same manner, the phase distribution in the case of N=6 using the first six lines of LED is shown in Fig. 11. In both of the distributions in the x-direction and the z-direction, the relationships are almost linear. Thus, the linearity is different according to the value N.

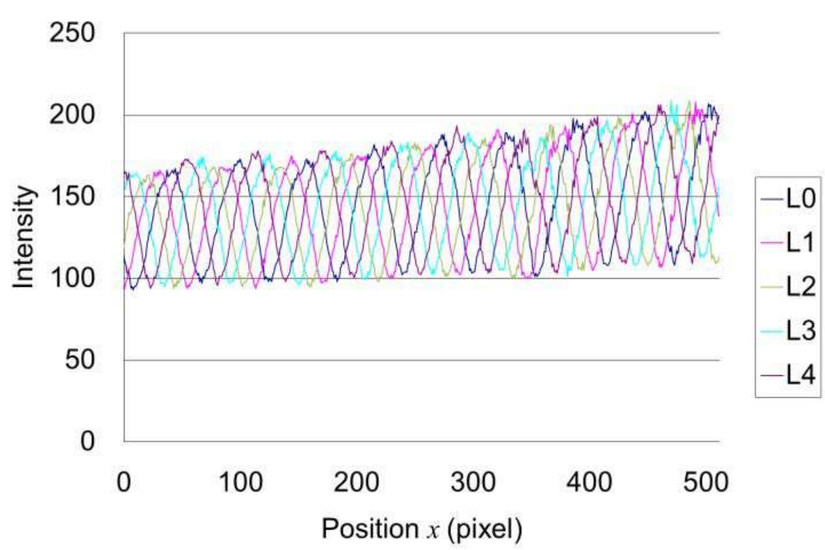

Fig. 9. Intensity distributions along x-axis of projected grating on reference plane when changing light sources

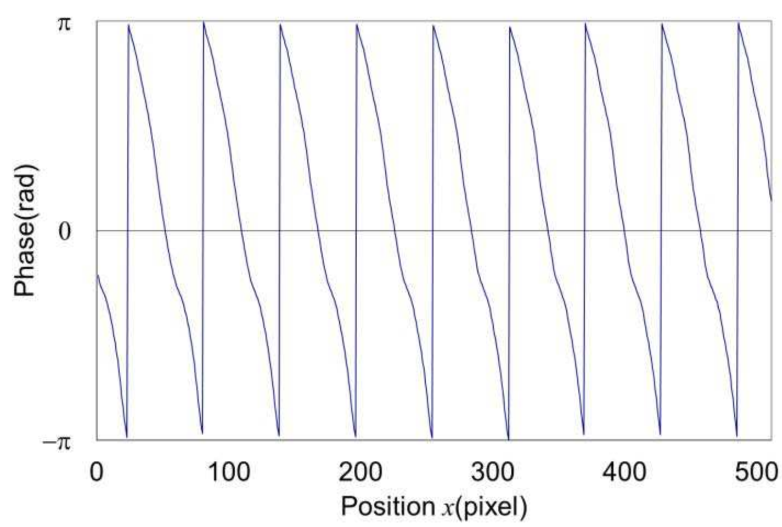

(a)

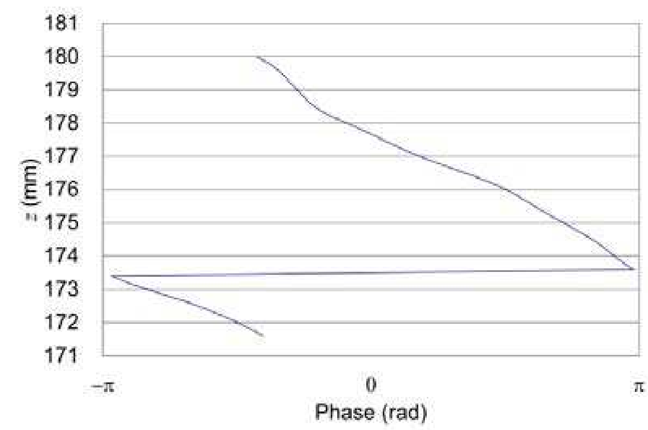

(b)

Fig. 10. Phase distributions along x-direction and z-direction when phase calculation is performed using N=4; (a) *x*-directional phase distribution; (b) *z*-directional phase distribution

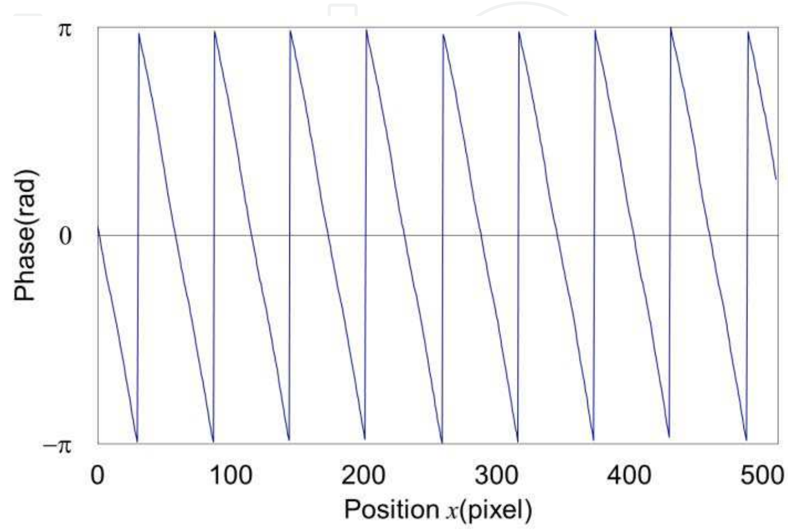

(a)

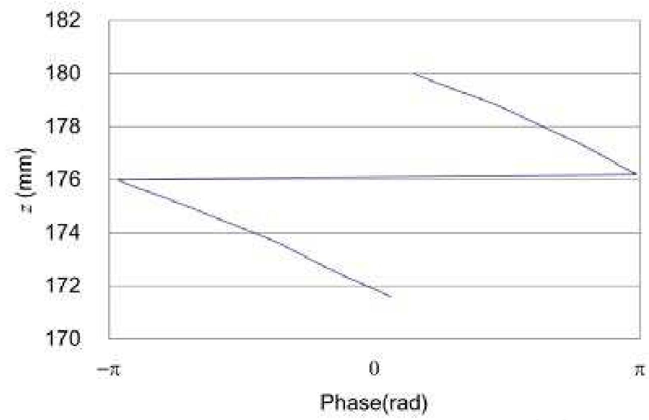

(b)

Fig. 11. Phase distributions along x-direction and z-direction when phase calculation is performed using N=6; (a) x-directional phase distribution; (b) z-directional phase distribution

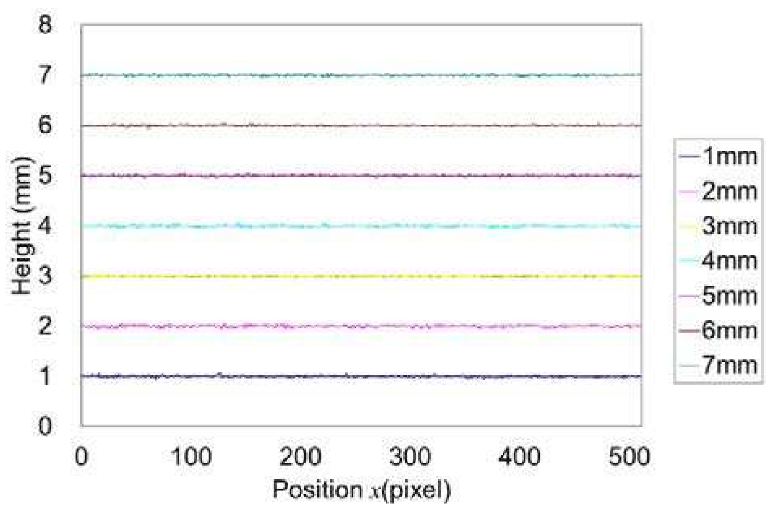

Fig. 12. Height distributions when the height is changed from reference plane at z=180mm (in case of N=4)

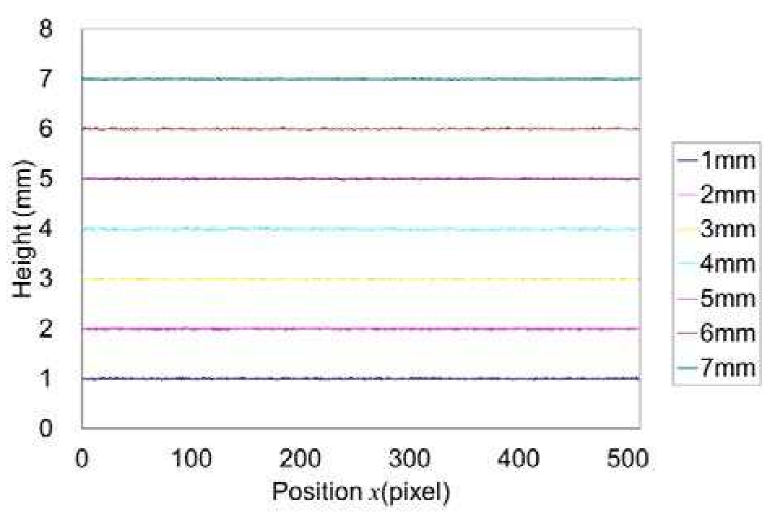

Fig. 13. Height distributions when the height is changed from reference plane at z=180mm (in case of N=6)

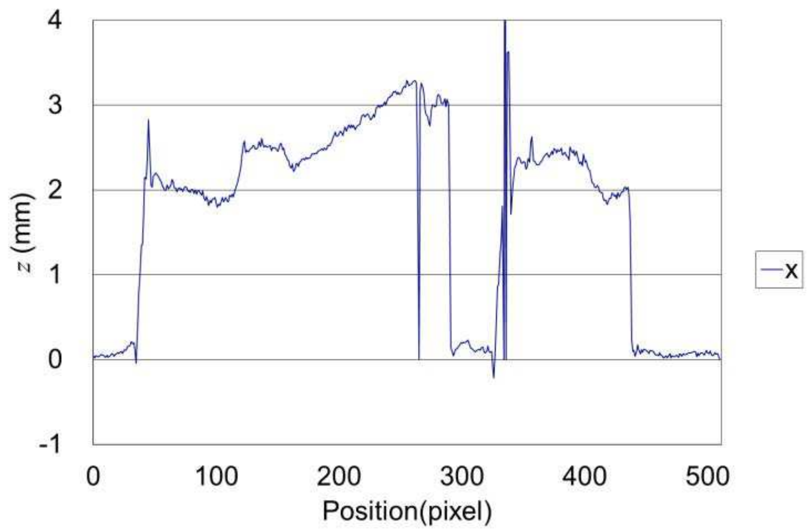

(a)

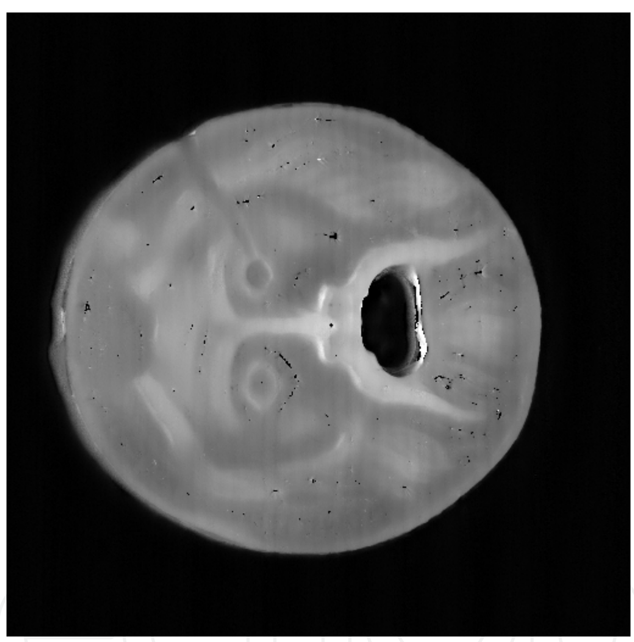

(b)

Fig. 14. Measurement result of mold of face; (a) Height distribution along center line; (b) Height distribution

Next, height measurement was performed. As the specimen, the reference plane was used. The results are shown in Figs. 12 and 13 and Tables 1 and 2. The average errors are less than 5 μm, and the standard deviations are 11~19 μm. Although the standard deviation in the case of N=6 is better than the one in the case of N=4, both have good accuracy.

As an example of shape measurement, the result of shape measurement of a face model cast is shown in Fig. 14. Although the measurement value shows unusual values in the edge part in small areas, almost all over the object is measured by the proposed method.

Height	1mm	2mm	3mm	4mm	5mm	6mm	7mm
Average	1.003	2.002	3.002	4.002	5.001	6.001	7.000
Error	0.003	0.002	0.002	0.002	0.001	0.001	0.000
Standard deviation	0.019	0.018	0.017	0.017	0.017	0.015	0.017

Table 1. Results of height measurement (in case of N=4)

Height	1mm	2mm	3mm	4mm	5mm	6mm	7mm
Average	1.005	2.003	3.004	4.002	5.001	6.002	7.000
Error	0.005	0.003	0.004	0.002	0.001	0.002	0.000
Standard deviation	0.013	0.013	0.012	0.012	0.012	0.012	0.011

Table 2. Results of height measurement (in case of N=6)

6. Conclusions

A new shape measurement method called phase-stepping method using multi-line LED light sources is proposed. A special LED array with nine line LEDs was developed. By using whole-space tabulation method (WSTM), a system using the multi-line LED light sources was developed. It could shift the phase of the projected grating easily. The principle and a system of the shape measurement using the phase stepping method using LEDs were shown. It was applied to three-dimensional shape measurement, and height has been measured with sufficient accuracy less than 20 μm. It is possible to make a high speed, high precision, low cost, small size and wide-dynamic range system. It also excludes lens distortion and intensity error of the projected grating in measurement results theoretically.

7. Acknowledgments

This study was supported by Hyogo COE Program Promotion Project financially. We appreciate the support.

8. References

Asundi, K. & Zhou, W. (1999a). Mapping Algorithm for 360-deg Profilometry with Time Delayed Integration Imaging, *Optical Engineering, 38,* pp. 339-344.

Asundi, A. & Wensen, Z. (1999b). Unified Calibration Technique and its Applications in Optical Triangular Profilometry, *Applied Optics, 38-16*, pp. 3556-3561.

Fujigaki M. & Morimoto, Y. (1996). Shape Measurement by Grid Projection Method without Influence of Aberration of Lenses, *Post Conference Proc. of the VIII International Congress on Experimental Mechanics SEM*, pp. 167-172.

Fujigaki M. & Morimoto, Y. (2003). Real-time Shape Measurement by Integrated Phase-Shifting Method Using Ronchi Grating, *Trans. Jpn. Soc. Mech. Eng., (in Japanese), 69-685, C*, pp. 2374-2380.

Fujigaki M. & Morimoto, Y. (2008a). Shape Measurement with Grating Projection Using Whole-Space Tabulation Method, *Journal of JSEM (in Japanese), 8-4*, pp. 92-98.

Fujigaki, M., Takagishi, A., Matui T. & Morimoto, Y. (2008b). Development of Real-Time Shape Measurement System Using Whole-Space Tabulation Method, *SPIE International Symposium, Proc. SPIE 7066*, 706606.

Fujigaki M., Masaya, A., Murakami, R. & Morimoto, Y. (2009). Accuracy Improvement of Shape Measurement Using Whole-Space Tabulation Method, *Proc. of ICEM2009 held in Singapore.*

Ha, T., Takaya, Y. & Miyoshi, T. (2004). High-precision On-machine 3D Shape Measurement Using Hypersurface Calibration Method, *Proc. SPIE, 5603*, pp. 40-50.

Kato, J., Yamaguchi, I., T. Nakamura & Kuwashima, S. (1997). Video-rate Fringe Analyzer Based on Phase-shifting Electronic Moire Patterns, *Applied Optics*, Vol. 36, No. 32, pp. 8403-8412.

Morimoto, Y., Fujigaki M. & Toda, H. (1999). Real-Time Shape Measurement by Integrated Phase-Shifting Method, *Proc. of SPIE, Vol. 3744*, pp. 118-125.

Morimoto, Y., Fujigaki M. & Masaya, A. (2009). Shape Measurement by Grating Projection and Whole-space Tabulation Method, *Proc. of ISOT2009 held in Istanbul*

Morimoto, Y., M. Fujigaki, M. Masaya, A. & Amino, Y. (2010a). Shape Measurement by Whole-space Tabulation Method Using Phase-shifting LED Projector, *Proceedings of International Conference on Advanced Phase Measurement Methods in Optics and Imaging, Monte Verita, Locarno, Switzerland, 17 to 21 May.*

Morimoto, Y., Fujigaki, M. Masaya, A. & Oura，Y. (2010b). Shape Measurement by Light-stepping Method Using LEDs, *ISOT 2010 International Symposium on Optomechatronic Technologies, 25-27 October 2010, Toronto, Canada*

Ri, S., Fujigaki M. & Morimoto, Y. (2005). Phase Reliability Evaluation in Phase-shifting Method Using Fourier Transform for Shape Measurement, *Optical Engineering, 44-8*, 083601-1-8.

Shinke, A., Morimoto, Y. & Fujigaki, M. (2001). Development of Accurate Shape Measurement System Using Multiple Reference Planes, *Proceedings of APCFS & ATEM '01*, pp. 811-814.

Sitnik, R. & Kujawinska, M. (2002). Digital Fringe Projection System for Large-volume 360-deg Shape Measurement, *Optical Engineering, 41-2*, pp. 443-449.

Srinivasan, V., Liu, H. C. & Halioua, M. (1984). Automated phase-measuring profilometry of 3-D diffuse objects, *Appl. .Opt. 23*, pp. 3105-3108.

Srinivasan, V., Liu, H. C. & Halioua, M. (1985). Automated phase-measuring profilometry: a phase mapping approach,, *Appl. Opt. 24*, pp. 185-188.

Su, X., Song, W, Cao, Y. & Xiang, I. (2004). Phase-height Mapping and Coordinate Calibration Simultaneously in Phase-Measuring Profilometry, *Optical Engineering, 43*, pp. 708-712.

Takeda, M. & Mutoh, K. (1983). Fourier Transform Profilometry for the Automatic Measurement of 3-D Object Shapes, *Applied Optics, 22-24*, pp. 3977-3982.

Yen, H. N., Tsai D. M. & Yang, J. Y. (2006). Full-field 3-D measurement of solder pastes using LCD-based Phase Shifting Techniques, IEEE Transactions on Electronics Packaging Manufacturing, 29-1, pp. 50-57.

Zhou, W-S. & Su, X.-Y. (1994). A Direct Mapping Algorithm for Phase-measuring Profilometry," Journal of Modern Optics, 41-1, pp. 89-94.

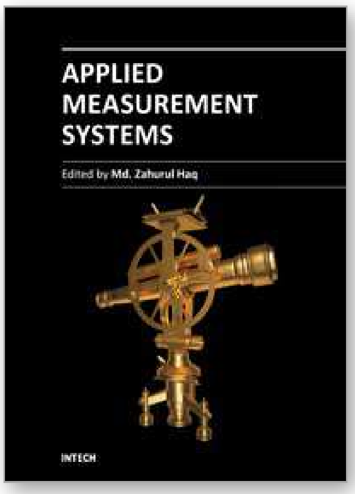

Applied Measurement Systems

Edited by Prof. Zahurul Haq

ISBN 978-953-51-0103-1

Hard cover, 390 pages

Publisher InTech

Published online 24, February, 2012

Published in print edition February, 2012

Measurement is a multidisciplinary experimental science. Measurement systems synergistically blend science, engineering and statistical methods to provide fundamental data for research, design and development, control of processes and operations, and facilitate safe and economic performance of systems. In recent years, measuring techniques have expanded rapidly and gained maturity, through extensive research activities and hardware advancements. With individual chapters authored by eminent professionals in their respective topics, Applied Measurement Systems attempts to provide a comprehensive presentation and in-depth guidance on some of the key applied and advanced topics in measurements for scientists, engineers and educators.